DOI: 10.7795/810.20200724

Li-ion batteries: characterization of the thermal runaway reactions using a DSC

Paola Russo [*], Maria Luisa Mele

[a] Department of Chemical Engineering Materials Environment, Sapienza University of Rome, Rome, Italy

E-mail: paola.russo@uniroma1.it

Abstract

Lithium-ion batteries are widely used in many applications due to their formidable performance and characteristics. Numerous accidents involving lithium-ion batteries have occurred in recent years and this has led to focus on safety issues related to their extensive use. In this work the Panasonic's NCR18650 lithium-ion cylindrical cells were investigated by Differential Scanning Calorimetry. The aim is to identify and characterize the main reactions that occur at the anode under thermal abuse conditions and which can lead to thermal runaway. The kinetics of these reactions are assessed using the Kissinger and Ozawa methods. Furthermore, the results show the relationship between the initial state of charge of the cell and the progress of reactions.

Keywords: *Thermal runaway, lithium-ion batteries, kinetics, fire, explosion.*

1. Introduction

Lithium-ion batteries are now widely used in many applications, particularly in portable digital electronics-based equipment or in the automotive sector for electric vehicles (EVs) due to their high-power density, long cycle life and low self-discharge (Tarascon et al., 2001; Ping et al., 2014; Garche et al., 2019).

Despite these advantages, this technology shows some safety problems related to thermal stability, which have led to numerous accidents occurred in recent years, for example in the automotive sector or in the energy storage sector (Bandhauer et al., 2011). The presence of dangerous substances both for humans and the environment, such as flammable organic solvents, lithium heavy metal oxides, carbon and lithium salts makes these devices potentially dangerous. The fire hazard of lithium-ion batteries is related to their chemical composition and conditions of use. In fact, during normal operating conditions a failure can occur, which can lead to the ignition of a thermal runaway, an unstoppable chain reaction during which a series of uncontrolled exothermic reactions occurs (Wang et al., 2012).

In a lithium-ion cell the negative electrode is protected by a film called Solid Electrolyte Interface (SEI). This film protects the electrode from direct reaction with solvent (Garche et al., 2019), but it is metastable and can decompose exothermically at 90–130 °C. Therefore, when the temperature rises to 70–90 °C decomposition begins of the SEI. The cell then starts self-heating followed by the exothermic reaction between intercalated lithium and electrolyte, and the exothermic reaction between the fluorinated binder and the lithiated carbon at high temperature (Du Pasquier et al., 1998; Spotnitz at al., 2003; Wang et al., 2006; Chen et al., 2011; Forestier et al., 2016).

The active cathode material can also decompose exothermically with the generation of oxygen which can react with the electrolyte by oxidizing it (Spotnitz at al., 2003; Belharouak et al., 2006).

 DOI: 10.7795/810.20200724

Therefore, it is necessary to evaluate the behaviour of lithium-ion batteries in abuse conditions that can help provide information for improving battery safety (Ruiz et al., 2018).

Furthermore, the development of a mathematical model to predict battery behavior in case of abuse requires knowledge of the mechanism of reactions that take place during the thermal runaway. On the other hand, it can help to reduce the number of tests to optimize the battery design.

Few studies have been carried out in the literature to evaluate the kinetic parameters of the main exothermic reactions that occur in batteries (Richard et al., 1999a, 1999b II), while others have determined the kinetic parameters of the decomposition reactions of negative and positive electrodes based on DSC tests (Wang et al., 2011), Geder, (2014), Yamaki et al., 2014; Chen et al., 2009).

In this framework this work is a preliminary study aimed at analyzing and characterizing the main reactions that occur at the anode during a thermal runaway. In particular, the mechanism of the SEI decomposition reaction (in the range 90-120 °C), which is the first step leading to a self-heating process, and of the reaction that occurs between the lithiated anode and the PVDF, which is the reaction that develops the greatest amount of heat. In addition, it is assessed how the state of charge of the batteries affects the reactions and their progress. For this purpose, the anode and cathode of the Panasonic's NCR 18650 cells in different states of charge are analyzed using a DSC.

2. Experiments

2.1 Materials

Panasonic's NCR18650 lithium-ion cylindrical cells (18 mm in diameter and 65 mm length) are tested. This type of cells is mostly used in the automotive sector. The active material for cathode is lithium-nickel-aluminum-cobalt oxide (NCA), while the anode is made of graphite. The binder is polyvinylidene fluoride (PVDF).

2.2 Charging procedure

Some cells are charged using a PS 8000 2U series power supply from Elektro-Automatik (EA) with a constant current of 12 A, imposing a maximum limit voltage of 4.2 V (accuracy <0.2%), which corresponds to a state of charge of the cell (SOC) equal to 100%. For other cells a maximum limit voltage of 3.7 V and 3.5 V has been set which corresponds to a SOC of 50% and 30%, respectively. SOC of 30% is the value at which lithium-ion cells are normally stored and transported.

2.3 Disassembly procedure

The cells are dismantled in a glovebox filled with argon and the collected materials are carefully sealed in sealed containers until the tests. To preserve the electrode system and not to upset it completely and to study the real system, the samples were tested including the current collector.

2.3 DSC tests

Hermetically sealed high pressure resistant stainless-steel pans are used to carry out the tests, in order to inhibit the leakage of the gaseous products formed during the test and avoid the danger of a catastrophic capsule breakage.

The mass of the samples is between 10-20 mg. The high-pressure capsules are crimped using a special sealing tool provided by the PerkinElmer, with fixed torque. All the tested samples are weighted before and after the experiment to test their effective hermetic closure.

 DOI: 10.7795/810.20200724

DSC measurements are performed using Perkin Elmer DSC equipment (model 8500) in nitrogen flow (20 mL min^{-1}) at different heating rate of 5, 7, 10, 15 K min^{-1} in the temperature range 25-350 K.

3. Results and discussion

The mechanisms of some processes are often too complicated and isoconversional methods are often used to describe their kinetics. Alternatively, the non-isothermal isoconversional methods described by Kissinger (1956) and Ozawa (1970) are applied to evaluate the pre-exponential factor (A) and the activation energy (E_a) of exothermic reactions when the mechanism is unknown. These methods are based on the basic assumption that the reaction rate to a given conversion is only a function of temperature (Vyazovkin et al., 1998).

The equations can be derived from the integration of the basic kinetic equation taking into account that the tests are performed in a non-isothermal way, during which the samples are heated at a constant heating rate: $\beta = dT / dt$.

From the results of the DSC tests carried out varying the heating rates, the Kissinger's equation can be written as follows:

$$ln\left(\frac{\beta_i}{T_{p,i}^2}\right) = ln\left(\frac{A_x R}{E_{a,x}}\right) - \frac{E_{a,x}}{RT_{p,i}} \qquad i = 1, 2, 3, \dots, u \tag{3.1}$$

where β_i is the heating rate, $T_{p,i}$ is the peak temperature, and u stands for the different values of the heating rate.

A $ln\left(\frac{\beta_i}{T_{p,i}^2}\right) vs \frac{1}{T_p}$ graph is then plotted, and the best-fit of experimental data is performed. The result is a straight line, the slope of which is the value of the activation energy $E_{a,x}$, while the pre-exponential factor A_x is obtained from the intercept.

In Ozawa method (Ozawa, 1970; Flynn et al. 1966, Flynn, 1983) the plot of $ln(\beta_i) vs \frac{1}{T_p}$ gives a straight line, the slope of which is:

$$\ln(\beta) \cong -0.4567 \frac{E}{R} \frac{1}{T_p} \tag{3.2}$$

while the pre-exponential factor A_x is obtained from the intercept.

Fig. 1, 2 and 3 show the results of DSC, in terms of specific heat vs temperature, of the tests performed on anode of cells with different states of charge (i.e. 30%, 50% and 100% of SOC, respectively) and heating rates.

DOI: 10.7795/810.20200724

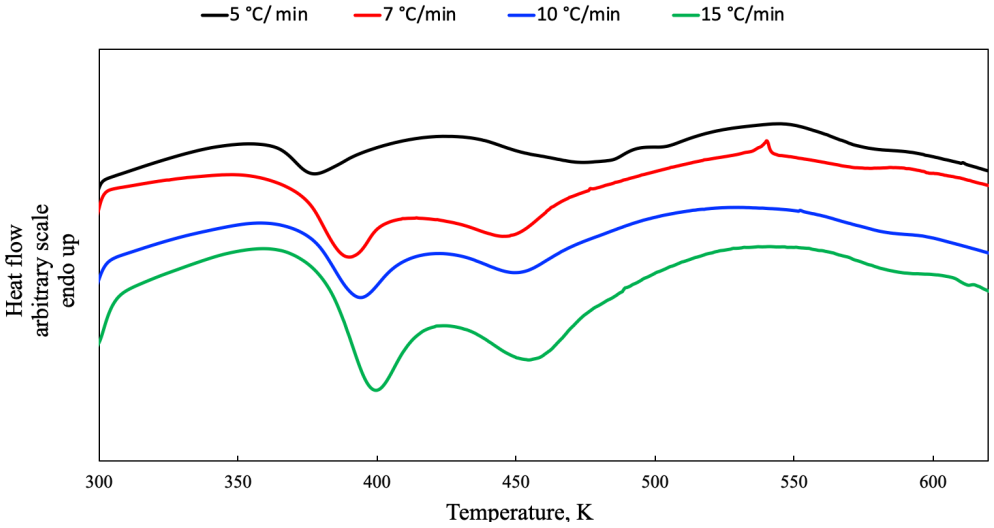

Fig. 1. *DSC curves at different heating rates of Panasonic NCR 18650 anode charged at 30% SOC*

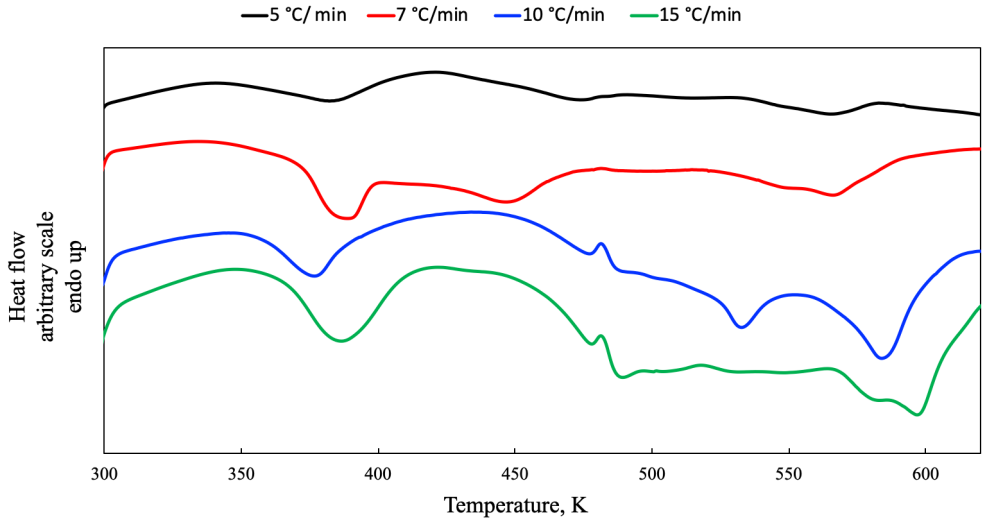

Fig. 2. *DSC curves at different heating rates of Panasonic NCR 18650 anode charged at 50% SOC*

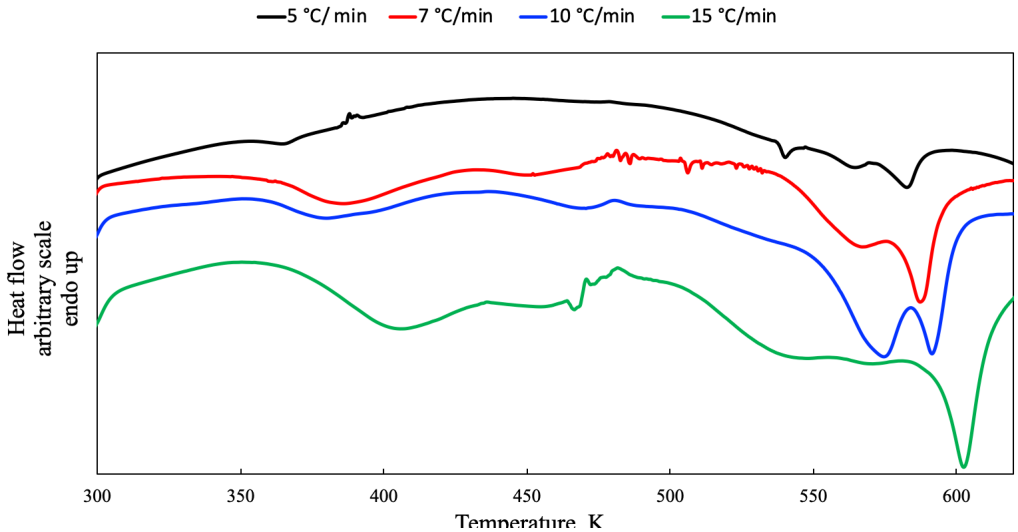

Fig. 3. *DSC curves at different heating rates of Panasonic NCR 18650 full charged*

 DOI: 10.7795/810.20200724

It appears that during heating two main exothermic reactions occur: i) the decomposition reaction of the SEI layer (104 – 130 °C) and the exothermic reaction between the lithiated anode and the PVDF binder (292 – 329 °C) (Du Pasquier et al., 1998).

Table 1 reports the peak temperatures of these reactions for cells at different states of charge

Table 1: *Peak temperatures of the exothermic reactions for cells at different states of charge*

Heating rate °C/min	30% SOC	50%SOC		100 %SOC		
	SEI decomposition	SEI decomposition	Li_xC_6-PVDF	SEI decomposition	Li_xC_6-PVDF 1st peak	Li_xC_6-PVDF 2nd peak
5	104.4 °C	108.9 °C	292.0 °C	92.2 °C	290.4°C	309.7 °C
7	115.7 °C	113.9 °C	294.2 °C	113.3 °C	290.8 °C	314.7 °C
10	120.3 °C	110.1 °C	311.3 °C	107.4 °C	300.5 °C	318.7 °C
15	125.5 °C	112.5 °C	324.8 °C	130.4 °C	/	329.5 °C

Standard uncertainty $\mathbf{u}(\mathbf{T}) = \pm 0.1$ K.

From fig. 1-3 it is possible to note that the presence and extent of the reaction between the lithiated anode and the binder is closely related to the state of charge of the cell. In detail, the lower SOC cell does not show a peak related to this reaction (Fig.1), while the 50% SOC cell shows only a smaller peak (Fig.2) than the double peaks visible in the results of the fully charged cell (Fig.3). In general, the use of different heating rate causes the temperatures at which reactions occur to shift, in particular, higher heating rates cause the reactions to move to higher temperatures. This is evident in all the figures. Furthermore, if different reactions occur in the same temperature range, the heat flux results may overlap and the peaks may not be resolved (Gabbott, 2008). This is evident in Fig.3 for the experiment conducted at heating rate of 15 °C/min in which a single peak appears at 329.5°C compared to other heating rate where two peaks are distinguished (1st peak at 290.4-300.5 °C , 2nd peak at 309.7-329.5 °C). Instead, the lower peak at 290-300 °C at lower SOC may be attributed to a low quantity and to the unavailability of lithium in the anode at that temperature (Roth et al., 2004). In fact, lithium and PVDF are not close each other, so lithium must diffuse through the graphite to reach PVDF and react, hence, not all the lithium is available for reaction. The more the degree of lithiation increases, which means that the higher the state of charge, the greater the quantity of lithium available for the reaction (Spotnitz et al., 2003).

In addition, fig.2 shows a small endothermic peak at around 200°C, probably due to the melting of the $LiPF_6$ (Roth et al., 1999). Beside this peak, DSC traces of pure $LiPF_6$ reported in literature also shows a greater endothermic decomposition peak at 285°C which is not evident in fig.2, which can be hidden by the exothermic peaks present in the same temperature range. The appearance of the endothermic peak only in fig.2 can be due to the different availability of $LiFP_6$ near the anode which is not always ensured in the sampling procedure used. Further studies will be conducted to confirm this hypothesis.

Table 2 reports the kinetic parameters calculated with both Kissinger and Ozawa methods. In particular, Fig.4 shows the method of calculating the kinetics parameters using Ozawa's method.

DOI: 10.7795/810.20200724

Table 2: *Kinetic parameters obtained from the Kissinger and Ozawa methods*

Sample	Reaction	A_x, s^{-1}		E_a, kJ mol^{-1}		R^2	
		Kissinger	Ozawa	Kissinger	Ozawa	Kissinger	Ozawa
30% SOC	**SEI decomposition**	2.1388×10^3	2.3744×10^9	56.50	137.78	0.91	0.93
50% SOC	**SEI decomposition**	1.2231×10^{42}	1.3310×10^{48}	340.03	758.01	0.89	0.89
	Li_xC_6-PVDF	1.0995×10^2	2.7492×10^8	73.49	181.90	0.93	0.95
100%SOC	**SEI decomposition**	2.9447	3.6953×10^5	27.93	75.07	0.87	0.91
	Li_xC_6-PVDF 1st peak	7.7594×10^7	1.8475×10^{14}	136.21	318.75	0.78	0.80
	Li_xC_6-PVDF 2nd peak	6.1677×10^{18}	1.6052×10^{15}	151.71	353.55	0.96	0.97

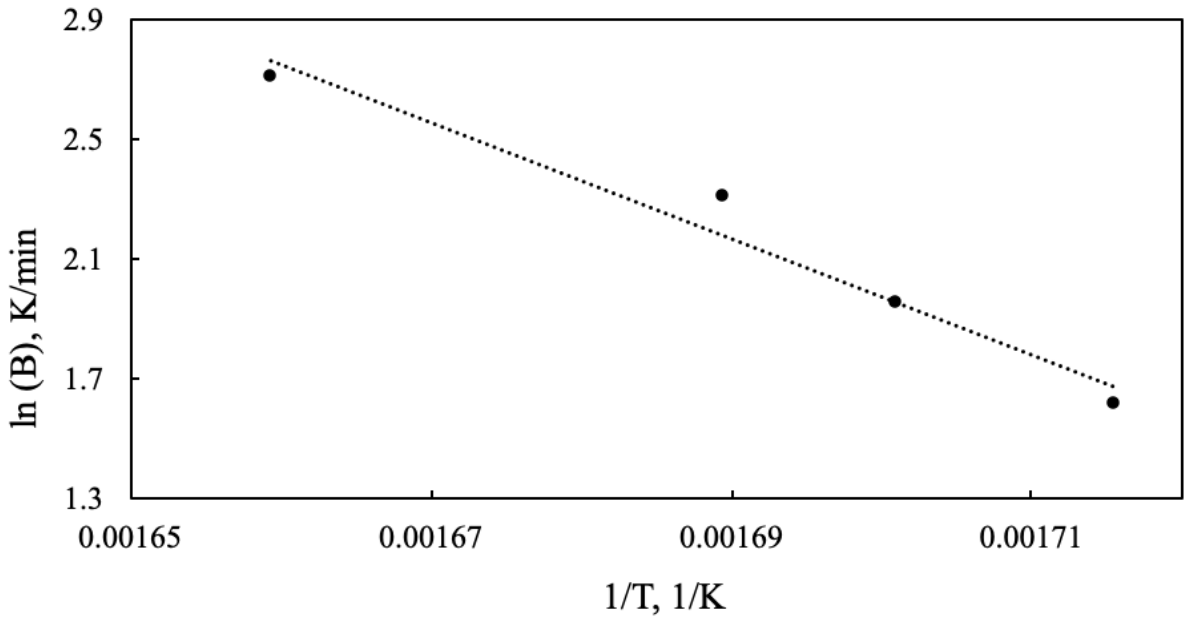

Fig. 4. *Ozawa's method for calculation of kinetics parameters for Li_xC_6-PVDF reaction (2nd peak) using (100% SOC)*

Analyzing the results, it is clear that the correlation coefficient is in the range 0.78-0.97. This means that the assumption of an Activation energy constant throughout the reaction is not exactly true (Flynn, 1983).

By comparing the data obtained with both methods, it is also found that the Ozawa method provides values with a higher correlation coefficient. Furthermore, the activation energy and the values of the pre-exponential factor of the Ozawa method agree well with those found in the literature (Ren et al., 2018).

 DOI: 10.7795/810.20200724

Conclusions

Panasonic's NCR 18650 lithium-ion cells have been tested using DSC tests at different heating rates. Two main exothermic reactions are recognized and analyzed: that at lower temperatures (104 – 130 °C) is related to the decomposition of the SEI and that, in the range 290-310°C, related to the reaction between the binder (PVDF) and the lithium intercalated in the negative electrode. These two reactions were kinetically analyzed using a non-isothermal isoconversional method developed by Kissinger and Ozawa.

The relationship between the initial state of charge of the cells and the reactions taking place is evident. As for to the SEI decomposition reaction, the activation energy for fully charged cells is significantly lower than for 30% and 50% state of charge.

The cells with lower SOC do not show the peak related to the Li_xC_6-binder reaction, while the cells with 50% SOC show only a minor peak, compared to the two peaks which is visible in the full charged cell. This is probably due to the availability of lithium during the tests, therefore the greater the state of charge and the greater the lithium available for the reaction.

The data obtained can be used as preliminary results for further and complementary analysis in order to develop a detailed mathematical model to describe all the reactions that occur during the thermal runaway.

Acknowledgements

The authors gratefully acknowledge the financial contribution from MISE-ENEA

References

Bandhauer T.M., Garimella S., Fuller T.F. (2011). A critical review of thermal issues in lithium-ion batteries. *Journal of the Electrochemical Society* 158 R1.

Belharouak I., Vissers D., Amine K. (2006). Thermal stability of the $Li(Ni_{0.8}Co_{0.15}Al_{0.05})O_2$ cathode in the presence of cell components. *Journal of the Electrochemical Society*; 153: A2030–5.

Chen Z., Qin Y., Liu J., Amine K. (2009). Lithium difluoro(oxalato)borate as additive to improve the thermal stability of lithiated graphite. *Electrochemical and Solid-State Letters*, 12: A69–72.

Chen Z., Qin Y., Ren Y., Lu W., Orendorff C., Roth E.P,. et al. (2011). Multi-scale study of thermal stability of lithiated graphite. *Energy & Environmental Science*, 4: 4023–30.

Du Pasquier A., Disma F., Bowmer T., Gozdz A. S., Amatucci G., Tarascon J. M. (1998). *Journal of the Electrochemical Society*, 145(2):472–477.

Flynn J.H. (1983). The Isoconversional Method for Determination of energy of Activation at Constant Heating rates, *Journal of Thermal Analysis and Calorimetry*, 27: 95-102.

Flynn J.H., Wall L.A. (1966). A Quick, Direct Method for the Determination of Activation energy from thermogravimetric Data, *Journal of Polymer Science Part C: Polymer Letters*, (4): 323-328.

Forestier C., Grugeon S., Davoisne C., Lecocq A., Marlair G., Armand M., et al. (2016). Graphite electrode thermal behavior and solid electrolyte interphase investigations: role of state-of-the-art

 DOI: 10.7795/810.20200724

binders, carbonate additives and lithium bis(fluorosulfonyl)imide salt. *Journal of Power Sources*, 330: 186–94.

Gabbott P., *Principles and Applications of Thermal Analysis*; Blackwell Publishing 2008.

Garche J., Brandt K. *Electrochemical Power Sources: Fundamentals, Systems, and Applications-Li-Battery Safety*; Elsevier 2019.

Geder J., Hoster H.E., Jossen A., Garche J., Yu D.Y.W. (2014). Impact of active material surface area on thermal stability of $LiCoO_2$ cathode. *Journal of Power Sources*, 257: 286–92.

Kissinger HE. (1956) Variation of peak temperature with heating rate in differential thermal analysis. *Journal of Research of the National Bureau of Standards,* 57: 217–21.

Ozawa T. (1970). Kinetic Analysis of Derivative Curves in thermal Analysis. *Journal of Thermal Analysis and Calorimetry*, (2):301-324.

Ping P., Wang Q., Huang P., Sun J., Chen C. (2014). Thermal behavior analysis of lithium ion battery at elevated temperature using deconvolution method. *Applied Energy*, 129: 261-73.

Ren D., Liu X., Feng X., Lu L., Ouyang M., Li J., He X. (2018). Model-based thermal runaway prediction of lithium-ion batteries from T kinetics analysis of cell components. *Applied Energy,* 228:633-644.

Richard M.N., Dahn J.R. (1999a). Accelerating rate calorimetry study on the thermal stability of lithium intercalated graphite in electrolyte. I. Experimental. *Journal of the Electrochemical Society*, 146: 2068–77.

Richard M.N., Dahn J.R. (1999b). Accelerating rate calorimetry study on the thermal stability of lithium intercalated graphite in electrolyte. II. Modeling the results and predicting differential scanning calorimeter curves *Journal of the Electrochemical Society*, 146: 2078–84.

Roth E. P., Doughty D. H., Franklin J. (2004). DSC investigation of exothermic reactions occurring at elevated temperatures in lithium-ion anodes containing PVDF-based binders. Journal of Power Sources 134: 222-234.

Roth E.P., Nagasubramanian G., Tallant D. R., Garcia M. (1999). Instability of polyvinylidene Fluoride-Based polymeric binder in lithium-ion cells: final report. Sandia Report SAND99-1164.

Ruiz V., Pfrang A., Kriston A., Omar N., Van den Bossche P., Boon-Brett L. (2018). A review of international abuse testing standards and regulations for lithium ion batteries in electric and hybrid electric vehicles. *Renewable and Sustainable Energy Reviews*, 81: 1427–52.

Simon P. (2004). Isoconversional methods - Fundamentals, meaning and application. *Journal of Thermal Analysis and Calorimetry*, Vol. 76: 123–132.

Spotnitz R., Franklin J. (2003). Abuse behavior of high-power, lithium-ion cells. *Journal of Power Sources*, 113:81–100.

Tarascon J. M., Armand M. (2001). Issues and challenges facing rechargeable lithium batteries. *Nature*, 414: 359-367.

 DOI: 10.7795/810.20200724

Vyazovkin S., Wight W. (1998). Isothermal and Non-isothermal kinetics of thermally Stimulated reactions of Solids, Int. Rev. Phys. Chem., 17(3), 407-433.

Wang Q., Sun J., Yao X., Chen C. (2006). Thermal behavior of lithiated graphite with electrolyte in lithium-ion batteries. *Journal of the Electrochemical Society*, 153: A329–33.

Wang H., Tang A., Huang K. (2011). Oxygen evolution in overcharge $Li_xNi_{1/3}Co_{1/3}Mn_{1/3}O_2$ electrode and its thermal analysis kinetics. *Chinese Journal of Chemistry*, 29: 1583–8.

Wang Q., Ping P., Zhao X., Chu G., Sun J., Chen C. Chen (2012). Thermal runaway caused fire and explosion of lithium ion battery. Journal of Power Sources, 208: 210–224.

Yamaki J., Shinjo Y., Doi T., Okada S. (2014). The rate equation for oxygen evolution by decomposition of Li_xCoO_2 at elevated temperatures. *Journal of the Electrochemical Society*, 161: A1648–54.